Comparison of PR Controller and Damped PR Controller for Grid Current Control of LCL Filter Based Grid-Tied Inverter under Frequency Variation and Grid Distortion

Ritwik Chattopadhyay, Ankan De
FREEDM Systems Centre, Department of ECE
North Carolina State University
Raleigh, NC, USA
email: rchatto@ncsu.edu

Subhashish Bhattacharya
FREEDM Systems Centre, Department of ECE
North Carolina State University
Raleigh, NC, USA
email: sbhatta4@ncsu.edu

Abstract— **Voltage Source Inverters (VSIs) are essential component for integration of renewable energy sources into utility grid or microgrid. Most of the utility grid regulation standards demand high quality sinusoidal current regulation by these inverters with renewable sources, which necessitates the use of LCL filters at the output of VSIs. Different load conditions and other factors influence grid conditions, such as voltage profile, harmonic distortion and frequency variation. The scope of this paper include comparison of effects on grid current of LCL filter based inverter while using PR controller and damped PR controller under distorted grid voltage and frequency variation conditions. The effects are analyzed through simulation studies in MATLAB/PLECS and real time simulation studies are carried out in Typhoon HIL environment.**

I. INTRODUCTION

With increasing demand for renewable electrical energy generation, grid connected inverters have become the main interface for integration of renewable energy sources into utility grid. Voltage source inverters using fast switching devices like Mosfets and IGBTs have high switching ripple component at the output voltage and current. Utility regulation prohibits any utility interface from feeding or drawing non-sinusoidal current to and from grid, allowing current profiles to have only the fundamental component of grid frequency. Three phase grid voltages generally possess fifth and seventh order harmonic components. The interfacing voltage source inverter for renewable energy sources needs to feed switching ripple free and harmonic free current into grid. As a method to reduce or eliminate the effect of switching ripple, different passive filters are used to reduce the effect of fifth and seventh order harmonics in grid voltage, extra control techniques need to be used.

Passive filters used for voltage source PWM inverters are mostly of two kinds L and LCL. L filters, generally of high value, act as impedance between inverter and grid and are able to block switching ripple components to some extent depending on the value of inductance. High value inductances at low frequencies(50/60 Hz) are generally bulky, heavy and made of silicon-steel laminated cores and create high losses. LCL filter possesses two small size inductors and a capacitor[1], and has the advantage of eliminating the switching ripple effect by bypassing the switching ripple components through the capacitor branch. LCL filter using two small size inductors and a capacitor, used for grid-tie voltage source inverters have high attenuation capability than L filters and results in much less losses as compared to L filter. However, LCL filter itself is a third order system the presence of low LC resonant frequency demands active or passive damping methods for elimination of effects of LC resonant frequencies, along with complex current control strategies for third order system. Active damping methods are generally more preferable than passive methods as the latter would incorporate high losses.

Over the years, researchers have developed different methods of grid current control of LCL filter based inverter using stationary reference frame(SRF) based control and synchronously rotating reference frame(SRRF) based control[1]-[7]. Using SRRF, it is possible to use PI controller for controlling grid current as PI controllers are suitable for regulating dc inputs as all currents and voltages appear as dc in SRRF[3],[7]. However, using SRRF based control with PI regulators, multi-loop controllers and higher number of sensors are required. PR controllers are suitable for regulating ac input quantities and single loop control of grid current along with grid harmonic rejection have been addressed in literature. Since PR controllers are tuned for a particular tuning frequency[2][4][5][6], any input signal of a different frequency would experience much lower gain if passed through PR controller[8]. For grid connected inverters, specially in case of microgrid applications, where variation of frequency is quite regular, PR controller based current control technique would not be enough to match the gain at varying frequency. Moreover, using grid harmonic rejection technique with PR controllers[2], grid currents are highly affected by frequency deviation, as for fundamental frequency variation of Δf, the frequency variation for n^{th} order harmonic is $n\Delta f$. Hence higher the harmonic, higher is the deviation from tuning frequency and lower is the gain. To eliminate this drawback of PR controller, a possible method is presented in [9], using PI controllers in dq domain for every grid harmonic in SRRF. But this control method is

quite complex, involves dq-transformation at every grid harmonic frequency and involves lot of feedforward signals. A second method would be to use PR controllers with damping such that the gain is sufficiently high for a much wider band of frequencies. The work presented in this paper focuses on the comparison of PR controllers and damped PR controllers.

II. System Modelling and Controller

A. Modelling of LCL filter

A schematic of three phase grid-tied inverter is shown in figure 1. The inverter system is meant for 3 ph, 480V/60Hz grid. The inverter is chosen to have a power rating of 50 kW. For 480V three phase line, the dc link voltage is chosen at a value of 800V. For withstanding 800V dc link, SiC three phase module CAS100H12AM1 of rating 1200V/100A are available. The switching frequency is chosen to be around 10 kHz. The inductor and capacitor values are L1=2 mH, L2=1 mH, C=25 µF. The LC cut-off frequency is around 1200 Hz. The block diagram of undamped LCL filter, passively damped and actively damped LCL filter are shown in figures 2, 3 and 4.

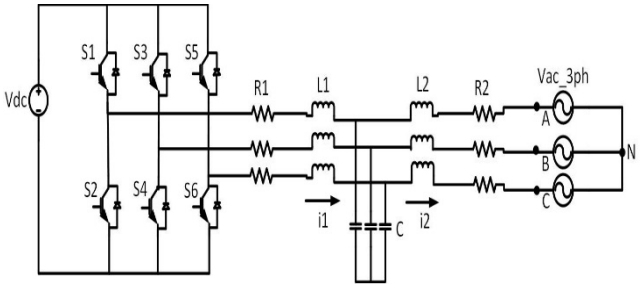

Fig.1. Three phase grid tied inverter with LCL filter

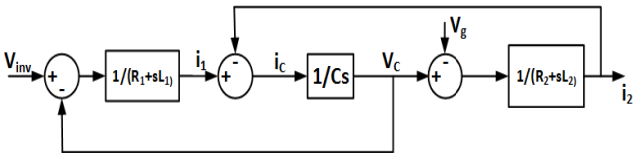

Fig.2. Block diagram of undamped LCL filter

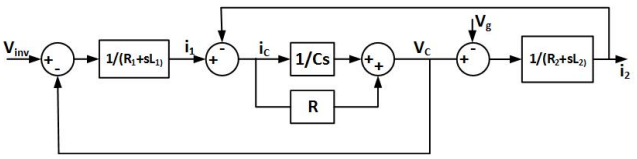

Fig.3. Block diagram of passively damped LCL filter

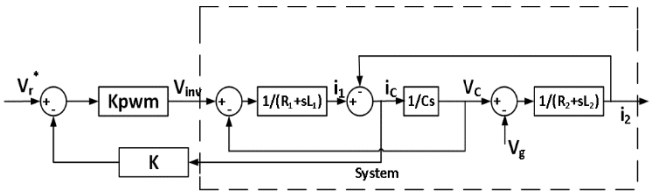

Fig.4. Block diagram of actively damped LCL filter

The transfer functions of outer current w.r.t. inverter voltage($G(i_2/V_{inv})$) are given by (1),(2) and (3). Figure 5 shows the frequency response of $G(i_2/V_{inv})$ for the three cases i.e. undamped, passively damped and actively damped. It can be observed that the LC oscillation peak at LC resonant frequency near 1200 Hz is sufficiently attenuated using passive damping or the active damping method[2] using capacitor current.

$$G_{un}(i_2/V_{inv})=\frac{1}{(s^3L_1L_2C+s^2(R_2L_1+R_1L_2)C+(R_1R_2C+L_1+L_2)s+R_1+R_2)} \quad [1]$$

$$G_p(i_2/V_{inv})=\frac{(RCs+1)}{(s^3L_1L_2C+s^2(RL_1+R_2L_1+RL_2)C+(RR_2C+L_1+L_2)s+R_1+R_2)} \quad [2]$$

$$G_a(i_2/V_{inv})=\frac{1}{(s^3L_1L_2C+s^2(RL_2+R_2L_1+KL_2)C+(RR_2C+KR_2C+L_1+L_2)s+R_1+R_2)} \quad [3]$$

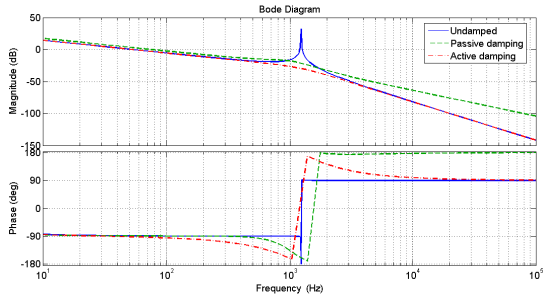

Fig.5. Frequency response of LCL filter

For grid current control of the LCL filter based inverter, it is necessary to analyze the grid impedance provided by the LCL filter and the controller used. Figure 6 shows the block diagram for closed loop grid current control of the inverter. Figure 7 shows the equivalent circuit of the LCL filter based inverter with the use of active damping. The grid impedance expression is derived by setting Vr*=0 in figure 6 and given in equation (4)[2].

$Z_{grid} = V_g / i_2$

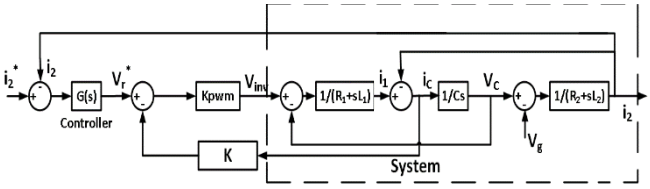

Fig.6. Closed loop block diagram of the System

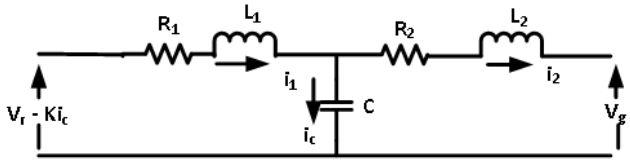

Fig.7. Equivalent circuit with active damping

$$Z_{grid}=-\left(\frac{s^3L_1L_2C+s^2(L_1R_2+R_1L_2+KL_2)C+s(R_1R_2C+KR_2C+L_1+L_2)}{s^2L_1C+KCs+R_1Cs+1}+\frac{R_1+R_2+G(s)}{s^2L_1C+KCs+R_1Cs+1}\right) \quad [4]$$

B. Comparison of PI, PR and Damped PR Controller

PR Controllers have significant advantage over PI controllers in terms of regulating ac input quantities. PI Controllers provide high gain over dc signals and need to have a very high bandwidth for accurately regulating ac signals. However, PI controllers are basically low pass filters hence they do provide a lag in case of regulating ac quantities. Moreover, it is not always possible to provide a very high bandwidth for PI controllers if switching frequency is not very high. While PR controllers are tuned to provide a very high gain or an infinite gain at the tuning frequency. PR controllers are very good at regulating a time varying ac periodic signal of fixed frequency. PR controllers have the disadvantage that if the input quantity to the controller has a frequency other than the tuning frequency of the PR controller, then the controller will provide a much lower gain and will not be able to regulate the reference signal. A sample bode plot of PI controller and a PR controller tuned at 60 Hz is shown in figure 7. The parameters are given as follows, Kp=25, Ki=Kr=1000.

$$G_{pi} = K_p + \frac{K_i}{s} \qquad [5]$$

$$G_{pr} = K_p + \frac{K_r s}{s^2 + \omega^2} \qquad [6]$$

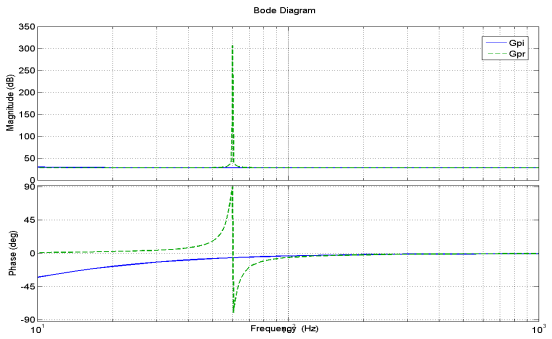

Fig.7. Bode plot of PI and PR controllers

It can be observed from figure 7 that PR controller is giving a very high gain at 60 Hz but at all other frequencies it is giving the same gain as PI controller. Hence it can be concluded that PI controller is capable enough for providing sufficient gain to ac input quantity of frequency 60 Hz. However, PR controller does provide a very high gain to ac input quantity of tuning frequency. To overcome the problem of this PR controller, PR controller with damping is considered which gives sufficient gain over a band of frequencies adjacent to tuning frequency. A comparison of PR controller tuned at 60 Hz and a damped PR controller of the form is shown in figure 8, Kr1=10^6 and ω_c=3 Hz.

$$G_{prd} = K_p + \frac{K_{r1} s}{s^2 + 2\omega_c s + \omega^2} \qquad [7]$$

It can be concluded that PI controllers can provide a high gain for dc quantities, while PR controllers of (6) provide very high gain at tuning frequency and damped PR controllers of the form in (7) can provide sufficient gain over a wider band of frequencies centered at tuning frequency.

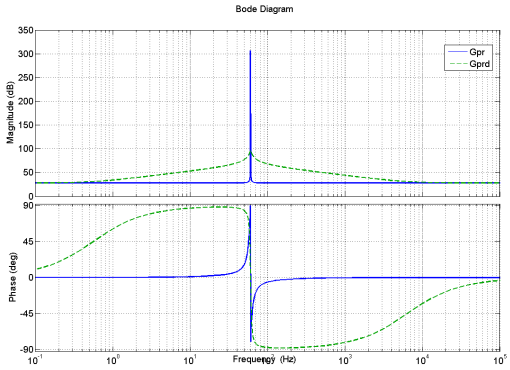

Fig.8. Bode plot of PR and damped PR controllers

III. Grid Impedance and Stability Analysis

A. Grid Imoedances with PR and Damped PR Controller

Grid current control of voltage source inverter demands sufficient grid impedance in order for proper controlling of grid current. High grid impedance at particular frequency ensures very small disturbance to grid current in case of grid voltage disturbance. The scope of the work mainly aims at the analysis of this grid impedance using PR controller and damped PR controller. Voltage source inverters fed from renewable energy sources need to supply ripple free and harmonics free sinusoidal current of fundamental frequency of grid voltage. As three phase grid voltages generally have fifth and seventh order harmonics, it is required for the controller to provide high gain at these harmonic frequencies such that grid impedance is sufficiently high at these frequencies. In order for the controller to provide high gain at fifth and seventh harmonic frequency of fundamental, PR controllers of harmonic frequencies are added to (6) and is of the form in (8)[2]. Similarly for damped PR controller, the controller for reducing harmonic effects is given in (9).

$$G_{pr\_hc}(s) = K_p + \frac{K_{r1} s}{s^2 + \omega_1^2} + \frac{K_{r5} s}{s^2 + \omega_5^2} + \frac{K_{r7} s}{s^2 + \omega_7^2} \qquad [8]$$

$$G_{prd\_hc}(s) = K_p + \frac{K_{r1} s}{s^2 + 2\omega_{c1} s + \omega_1^2} + \frac{K_{r5} s}{s^2 + 2\omega_{c5} s + \omega_5^2} + \frac{K_{r7} s}{s^2 + 2\omega_{c7} s + \omega_7^2} \qquad [9]$$

In equations (8) and (9), ω_1=120π rad/s, ω_5=5*ω_1, ω_7=7*ω_1, ω_{c1}=ω_1/20, ω_{c5}=ω_5/20, ω_{c7}=ω_7/20. Using (8) and (9) in equation (4), we get the grid impedance expression in (10) using PR controller[2] and grid impedance using damped PR controller in (11). Figure 9 shows the bode plot of Z_{grid_pr} and Z_{grid_prd}.

$$Z_{grid\_pr} = -\left(\begin{array}{l} \frac{s^3 L_1 L_2 C + s^2 (L_1 R_2 + R_1 L_2 + K L_2) C}{s^2 L_1 C + K C s + R_1 C s + 1} \\ + \frac{s(R_1 R_2 C + K R_2 C + L_1 + L_2) + R_1 + R_2}{s^2 L_1 C + K C s + R_1 C s + 1} \\ + \frac{1}{s^2 L_1 C + K C s + R_1 C s + 1} (K_p + \frac{K_{r1} s}{s^2 + \omega_1^2} + \frac{K_{r5} s}{s^2 + \omega_5^2} + \frac{K_{r7} s}{s^2 + \omega_7^2}) \end{array} \right) \qquad [10]$$

$$Z_{grid\_prd} = -\left(\begin{array}{l} \dfrac{s^3L_1L_2C + s^2(L_1R_2 + R_1L_2 + KL_2)C}{s^2L_1C + KCs + R_1Cs + 1} \\ + \dfrac{s(R_1R_2C + KR_2C + L_1 + L_2) + R_1 + R_2}{s^2L_1C + KCs + R_1Cs + 1} \\ + \dfrac{1}{s^2L_1C + KCs + R_1Cs + 1}(K_p + \dfrac{K_{r1}s}{s^2 + 2\omega_{c1}s + \omega_1^2} \\ + \dfrac{K_{r5}s}{s^2 + 2\omega_{c5}s + \omega_5^2} + \dfrac{K_{r7}s}{s^2 + 2\omega_{c7}s + \omega_7^2}) \end{array}\right) \quad [11]$$

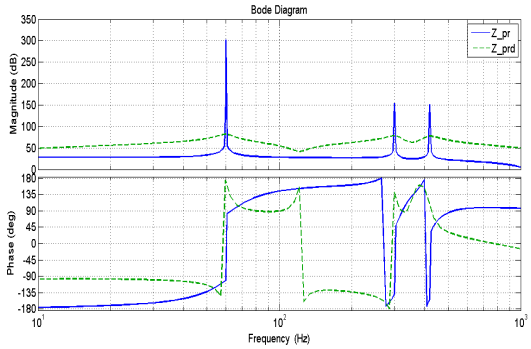

Fig.8. Bode plot of grid impedances

From figure 8, it can be observed that though PR controllers provide very high impedance for grid current at tuning frequency, damped PR controllers can be tuned to provide sufficient impedance for eliminating grid disturbance effects and harmonics.

B. Stability Analysis of LCL filter with PR and Damped PR Controller

Voltage source inverters with LCL filter, feeding power into grid, must act as a stable system. In order to find out the stability of the system, it is required to analyze the system poles and zeros, which depend on the system parameters. For actively damped system of figure 6, the open loop gain of the system is given as $G_{pr\_hc}(s)*G_a(s)$ and $G_{prd\_hc}(s)*G_a(s)$ where $G_a(s)$ is from equation 3 and $G_{pr\_hc}(s)$ and $G_{prd\_hc}(s)$ are from equations 8 and 9.

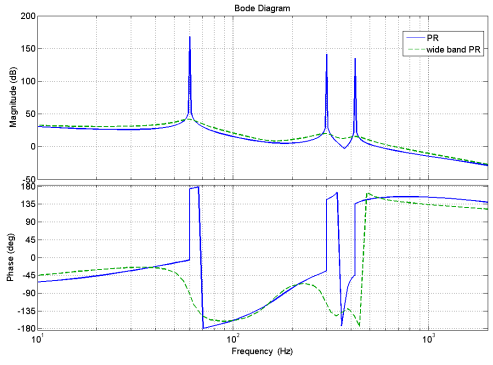

Fig.9. Open loop system bode plot with PR and damped PR controllers

PR controllers provide infinite gain at tuning frequency, but damped PR controller parameters need to be tuned to provide sufficient gain at tuning frequency. For PR controller of equation 8, K_p=20, K_{r1}=5000, K_{r5}=10000, K_{r7}=10000. For damped PR controller of equation 9, K_p=6, K_{r1}=6200, K_{r5}=15000, K_{r7}=20000. Figure 9 shows the bode plot of open loop gain of the system $G_{pr\_hc}(s)*G_a(s)$ and $G_{prd\_hc}(s)*G_a(s)$.

It is necessary to analyze the effect of system or control parameter variations over the stability of the system. For the scenario of figure 6, the parameter that is configurable is the active damping gain K, which can have different impacts on the stability of the system depending on its value. Figure 10 shows the s-plane pole-zero plot of the dominant poles and zeroes for the closed loop system for K=4, which makes the system unstable as it has two poles on right hand side of jω axis.

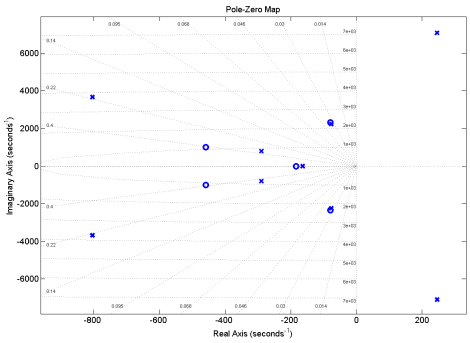

Fig.10. Closed loop system pole zero plot with PR controller(K=4)

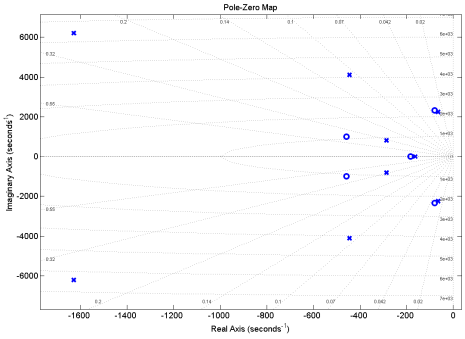

Fig.11. Closed loop system pole zero plot with PR controller(K=10)

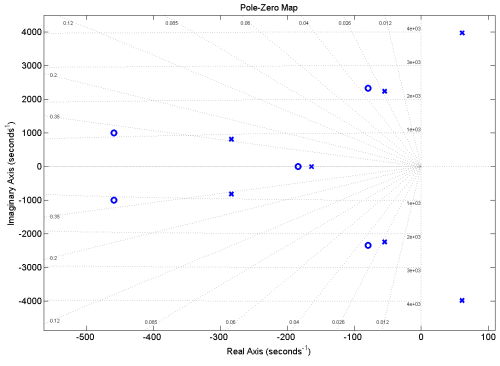

Fig.12. Closed loop system pole zero plot with PR controller(K=16)

As we increase the value of K to 10, the system has all the poles in the left hand side of jω axis(figure 11). As we further go on increasing the value of K, a pair of complex

conjugate poles again move on to the right hand plane(figure 12). Hence some value of K(around 10) which enables all the poles of the closed loop system to be on the left half s-plane is chosen. Similarly, for damped PR controller as well, variation of K, affects the closed loop system poles. Figure 13, 14, 15 shows the variation of system closed loop poles with variation in K.

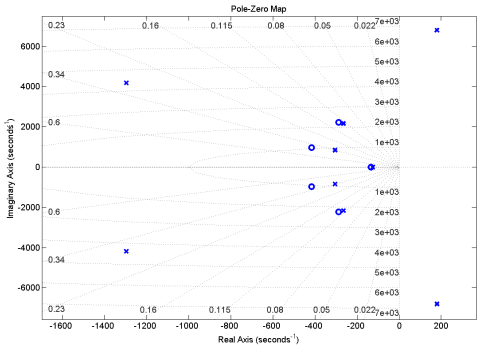

Fig.13. Closed loop system pole zero plot with damped PR controller(K=4)

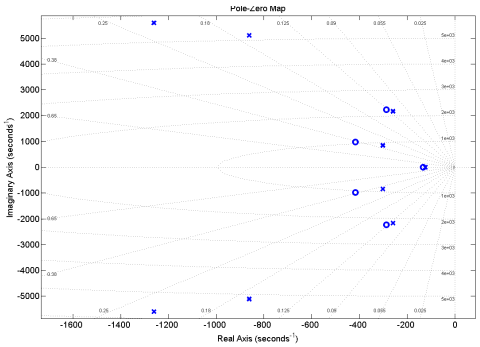

Fig.14. Closed loop system pole zero plot with damped PR controller(K=9)

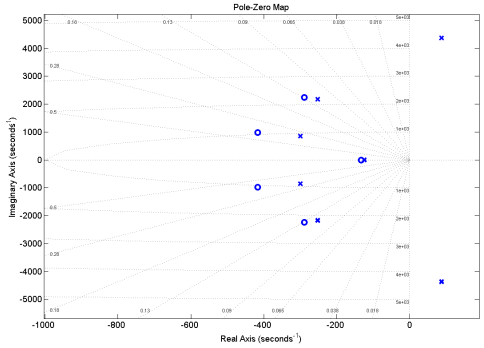

Fig.15. Closed loop system pole zero plot with damped PR controller(K=16)

IV. Results and Discussions

A. Simulation Study

To analyze the effect of PR controller and damped PR controller on the grid current control of LCL filter bases voltage source inverter, a MATLAB/SIMULINK model of the system shown in figure 1 has been built. The parameter values for the inductor and capacitors are chosen as given in section II. The controller gain and damping factors are chosen according to section III. The three phase grid current control has been achieved in α-β stationary reference frame. The overall control block diagram is shown in figure 16. For the simulation study, a variation of +/- 2Hz is considered. The grid voltage has 8% fifth and seventh harmonics. Figures 17,18,19 show the grid voltage and grid current profile using PR controller at 60Hz, 58Hz and 62Hz.

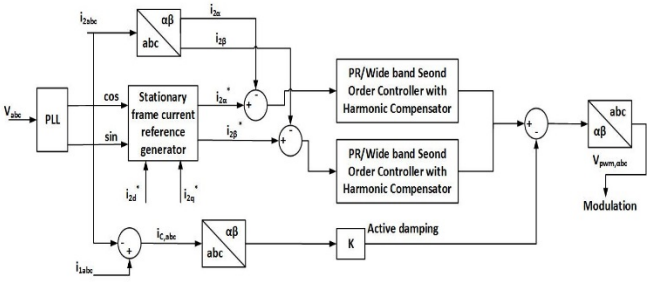

Fig.16. Control block diagram in α-β stationary reference frame for three phase grid tied inverter

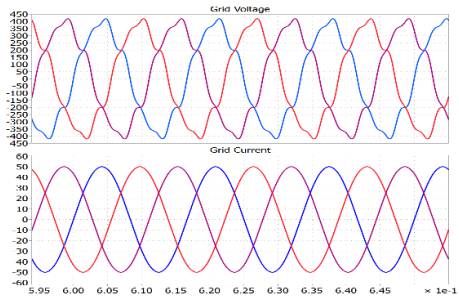

Fig.17. Grid voltage and grid current using PR controller at 60Hz.

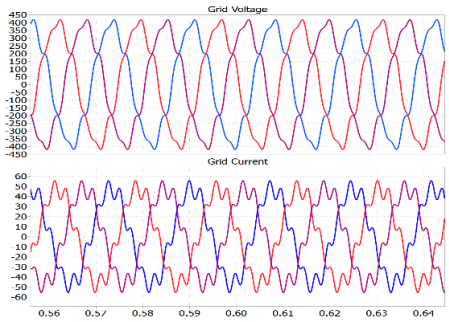

Fig.18. Grid voltage and grid current using PR controller at 58Hz.

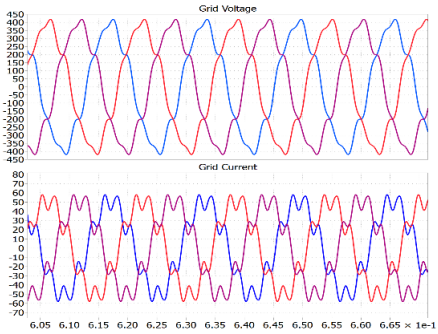

Fig.19. Grid voltage and grid current using PR controller at 62Hz.

It is evident from figure 18 and 19 that if frequency varies, PR controller is not able to provide high impedance towards grid using the current control described in section

III. Hence in order to provide a high grid impedance at varying frequency, grid current control of the system is analyzed using damped PR controllers. Figures 20, 21, 22 show the grid current profile using damped PR controller at different frequencies, which show the grid current to be devoid of grid harmonics. To verify these approach of eliminating grid harmonic effects over varying frequency range, real time simulation study in hardware-in-loop platform is presented in part B of this section.

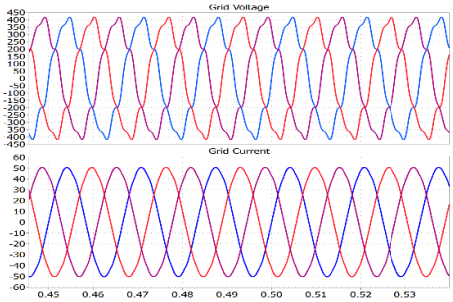

Fig.20. Grid voltage and grid current using damped PR controller at 60Hz.

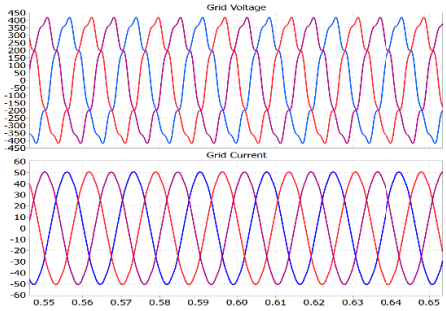

Fig.21. Grid voltage and grid current using damped PR controller at 58Hz.

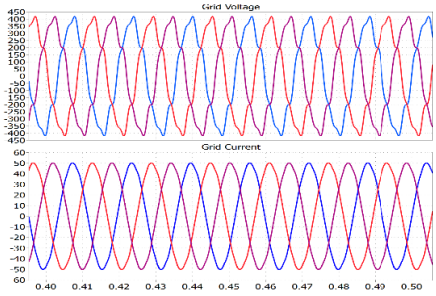

Fig.22. Grid voltage and grid current using damped PR controller at 62Hz.

B. Real Time Simulation Study in Hardware-in-Loop

Real time simulation study of the system shown in figure 1 has been carried out in Typhoon HIL400 real time simulator platform using TMS320F28335 DSP as the controller for the inverter. A diagram for the HIL setup is shown in figure 23. An inverter module has been developed in Typhoon HIL software and the compiled module is then loaded into the HIL400 hardware. The DSP is externally connected to Typhoon HIL400 though a docking station. The analog signals(voltages and currents) from the inverter module inside HIL is sensed by the ADC embedded with DSP and required PWM signals are generated. The PR and damped PR controllers are modeled in DSP in discrete form using bilinear transformation as given in [10], using timestep T_s=25 µS. The resonant part of PR and damped PR controller models are shown in (12) and (13), where ω is the tuning frequency of the controller.

$$G_{pr}(z)=\frac{2K_rT_s(1-z^{-2})}{(4+w^2T_s^2)+(2w^2T_s^2-8)z^{-1}+(4+w^2T_s^2)z^{-2}} \quad [12]$$

$$G_{pr\_d}(z)=\frac{2K_rT_s(1-z^{-2})}{(4+4\omega_cT_s+w^2T_s^2)+(2w^2T_s^2-8)z^{-1}+(4-4\omega_cT_s+w^2T_s^2)z^{-2}} \quad [13]$$

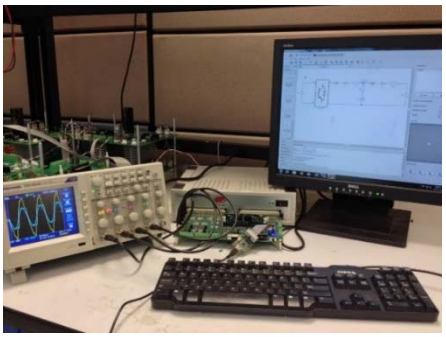

Fig.23. Real time simulation setup in Typhoon HIL400

In the HIL400 setup the inverter module performance using PR controller and damped PR controller are analyzed. Figures 24(a)-(d), 25(a)-(d), 26(a)-(d) show the grid current control using PR controller for peak currents of 50A, 20A and 10A respectively. Table 1, 2 and 3 show the percentage of harmonics for the three current levels at different frequencies. It can be observed from the figures and tables that as the current gets lower and frequency varies, the effects of grid harmonics are more prominent and the percentage of harmonics in grid current increases.

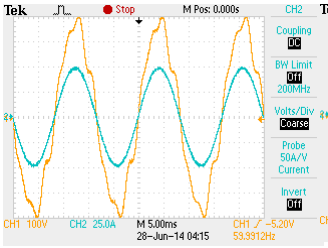

Fig. 24(a). Grid voltage and current at 60 Hz(50A)

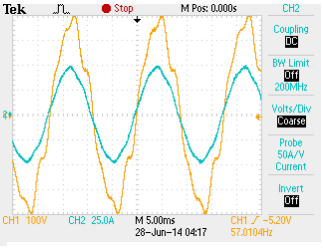

Fig. 24(b). Grid voltage and current at 57 Hz(50A)

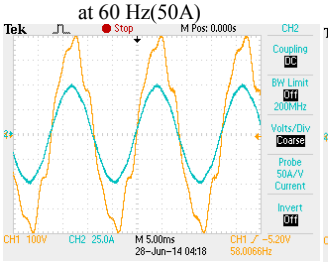

Fig. 24(c). Grid voltage and current at 58 Hz(50A)

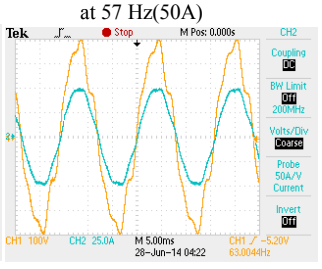

Fig. 24(d). Grid voltage and current at 63 Hz(50A)

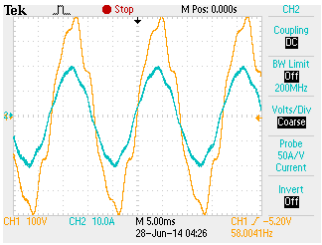

Fig. 25(a). Grid voltage and current at 58 Hz(20A)

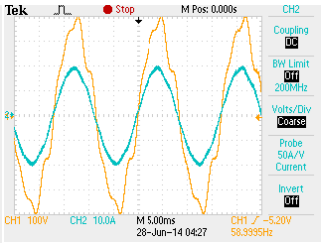

Fig. 25(b). Grid voltage and current at 59 Hz(20A)

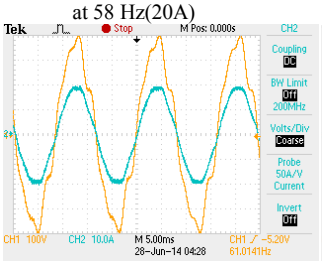

Fig. 25(c). Grid voltage and current at 61 Hz(20A)

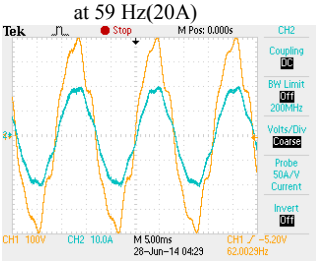

Fig. 25(d). Grid voltage and current at 62 Hz(20A)

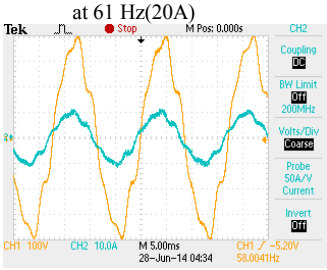

Fig. 26(a). Grid voltage and current at 58 Hz(10A)

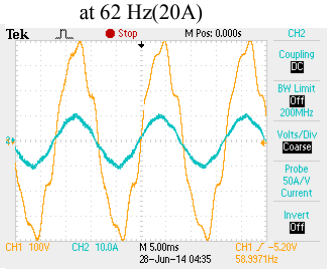

Fig. 26(b). Grid voltage and current at 59 Hz(10A)

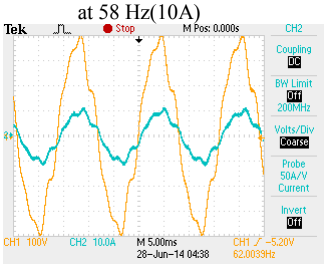

Fig. 26(c). Grid voltage and current at 62 Hz(10A)

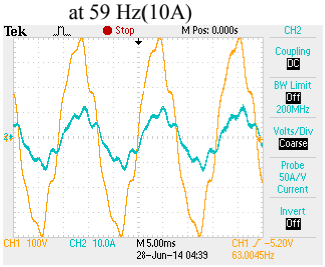

Fig. 26(d). Grid voltage and current at 63 Hz(10A)

TABLE 1. GRID CURRENT HARMONICS WITH PR CONTROLLER

50 A peak current (percentage of 5th and 7th w.r.t. fundamental component)							
Freq	57Hz	58Hz	59Hz	60Hz	61Hz	62Hz	63Hz
5th	1.46%	0.83%	0.34%	0.1%	0.95%	1.67%	2.67%
7th	2.48%	1.57%	0.72%	0.02%	1.06%	1.95%	3%

TABLE 2. GRID CURRENT HARMONICS WITH PR CONTROLLER

20 A peak current (percentage of 5th and 7th w.r.t. fundamental component)							
Freq	57Hz	58Hz	59Hz	60Hz	61Hz	62Hz	63Hz
5th	4.04%	2.66%	1.25%	0.14%	1.9%	3.5%	5.8%
7th	6.3%	4.13%	2%	0.15%	2.23%	4.5%	6.9%

TABLE 3. GRID CURRENT HARMONICS WITH PR CONTROLLER

10 A peak current (percentage of 5th and 7th w.r.t. fundamental component)							
Freq	57Hz	58Hz	59Hz	60Hz	61Hz	62Hz	63Hz
5th	7.47%	5.11%	2.49%	0.18%	3.66%	7.3%	10.9%
7th	12%	7.8%	4%	0.16%	4.3%	9%	13%

Using damped PR controller, figures 27(a)-(d), 28(a)-(d), 29(a)-(d) show the grid current control performance for peak currents of 50A, 20A and 10A respectively. Table 4, 5 and 6 show the percentage of harmonics for the three current levels at different frequencies. It can be observed that the percentage of harmonics in grid current for different currents and at different frequencies are much lesser than that using PR controller. The percentage of harmonics in current using damped PR Controller are 8-10 times lower than those using PR controller.

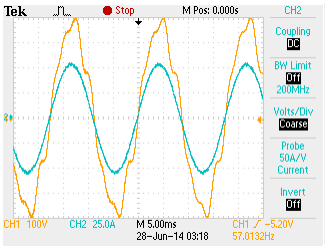

Fig. 27(a). Grid voltage and current at 57 Hz(50A)

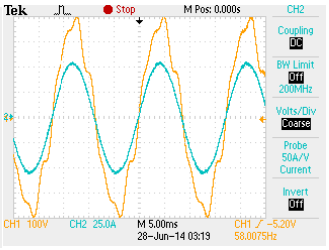

Fig. 27(b). Grid voltage and current at 58 Hz(50A)

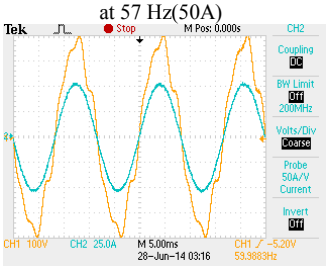

Fig. 27(c). Grid voltage and current at 60 Hz(50A)

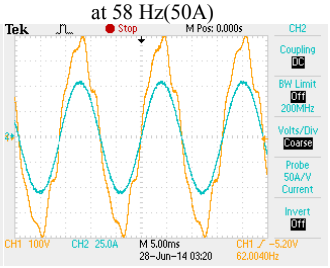

Fig. 27(d). Grid voltage and current at 62 Hz(50A)

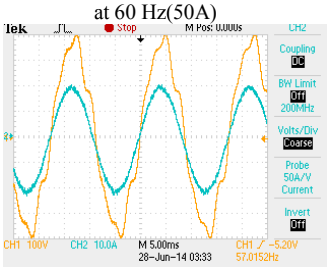

Fig. 28(a). Grid voltage and current at 57 Hz(20A)

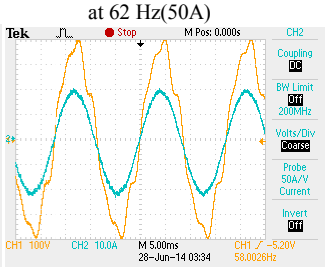

Fig. 28(b). Grid voltage and current at 58 Hz(20A)

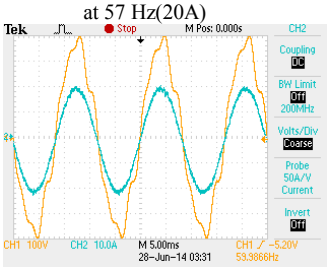

Fig. 28(c). Grid voltage and current at 60 Hz(20A)

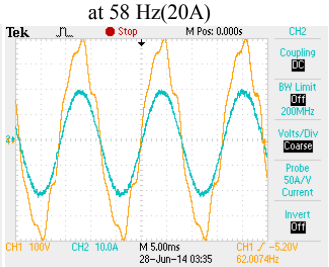

Fig. 28(d). Grid voltage and current at 62 Hz(20A)

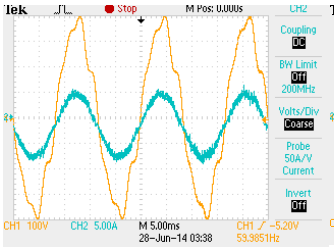

Fig. 29(a). Grid voltage and current at 60 Hz(10A)

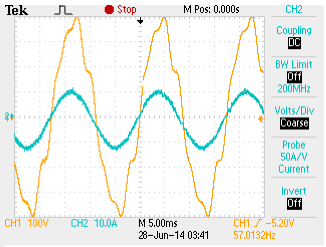

Fig. 29(b). Grid voltage and current at 57 Hz(10A)

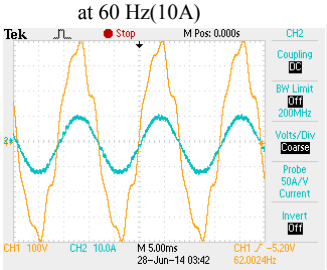

Fig. 29(c). Grid voltage and current at 62 Hz(10A)

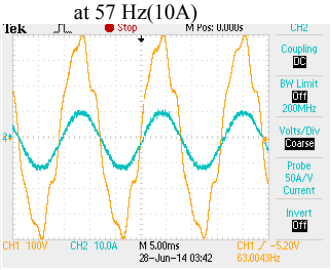

Fig. 29(d). Grid voltage and current at 63 Hz(10A)

TABLE 4. GRID CURRENT HARMONICS WITH DAMPED PR CONTROLLER

50 A peak current (percentage of 5th and 7th w.r.t. fundamental component)							
Freq	57Hz	58Hz	59Hz	60Hz	61Hz	62Hz	63Hz
5th	0.33%	0.3%	0.3%	0.26%	0.28%	0.33%	0.35%
7th	0.55%	0.52%	0.5%	0.44%	0.52%	0.57%	0.65%

TABLE 5. GRID CURRENT HARMONICS WITH DAMPED PR CONTROLLER

20 A peak current (percentage of 5th and 7th w.r.t. fundamental component)							
Freq	57Hz	58Hz	59Hz	60Hz	61Hz	62Hz	63Hz
5th	0.66%	0.64%	0.62%	0.43%	0.65%	0.67%	0.69%
7th	0.75%	0.75%	0.74%	0.58%	0.76%	0.78%	0.79%

TABLE 6. GRID CURRENT HARMONICS WITH DAMPED PR CONTROLLER

10 A peak current (percentage of 5th and 7th w.r.t. fundamental component)							
Freq	57Hz	58Hz	59Hz	60Hz	61Hz	62Hz	63Hz
5th	0.69%	0.67%	0.65%	0.45%	0.68%	0.72%	0.74%
7th	0.77%	0.76%	0.75%	0.58%	0.8%	0.82%	0.83%

V. CONCLUSIONS

From the above analysis and results, it is inferred that damped PR controllers are more suitable for grid current control of grid connected inverter, if grid voltage has harmonics in it and the fundamental frequency variation of grid voltage is there. Damped PR Controllers with proper gain adjustments do provide high gain over a frequency range adjacent to tuning frequency and thus can eliminate the effect of grid harmonics if frequency varies. Proper choice of gain of the controllers and tuning of the gain for active damping signal is necessary.

ACKNOWLEDGMENT

This work made use of FREEDM ERC shared facilities supported by National Science Foundation under award no. EEC-0812121.

REFERENCES

[1] M. Liserre, F. Blaabjerg, and S. Hansen, "Design and control of an LCLfilter-based three-phase active rectifier," *IEEE Trans. Ind. Appl.*, vol. 41, no. 5, pp. 1281–1291, Sep. 2005.

[2] Yaoqin Jia, Jiqian Zhao, Xiaowei Fu, "Direct Grid Current Control of LCL-Filtered Grid-Connected Inverter Mitigating Grid Voltage Disturbance", IEEE Transactions On Power Electronics, vol. 29, Issue 3, pp. 1532-1541, 2014.

[3] C. Wessels, J. Dannehl, and F. W. Fuchs, "Active damping of LCL-filter resonance based on virtual resistor for PWM rectifiers—Stability analysis with different filter parameters," in *Proc. IEEE Power Electron. Spec. Conf.*, 2008, pp. 3532–3538.

[4] G. Q. Shen *et al.*, "A New current feedback PR control strategy for gridconnected VSI with an LCL filter," in *Proc. IEEE Appl. Power Electron. Conf. Expo.*, Washington, DC, USA, 2009, pp. 1564–1569.

[5] E. Twining and D. G. Holmes, "Grid current regulation of a three-phase voltage source inverter with an LCL input filter," *IEEE Trans. Power Electron.*, vol. 18, no. 3, pp. 888–895, May 2003.

[6] Mohamed, Y.A.-R.I., "Mitigation of Dynamic, Unbalanced, and Harmonic Voltage Disturbances Using Grid-Connected Inverters With LCL Filter," *IEEE Trans. Ind. Electron.*, vol. 58, issue. 9, pp. 3914–3924, 2011.

[7] S.A. Khajehoddin, M. Karimi-Ghartemani, P.K. Jain, A. Bakhshai, "A Control Design Approach for Three-Phase Grid-Connected Renewable Energy Resources," *IEEE Trans. Sustainable Energy.*, vol. 2, issue. 4, pp. 423–432, 2011.

[8] Jin Huang, Yang Lu, Bo Zhang, Na Wang, Wensheng Song, "Harmonic current elimination for single-phase rectifiers based on PR controller with notch filter," *15th International Conference on Electrical Machines and Systems (ICEMS)*, pp. 1–5, 2012.

[9] S. Madhusoodhanan, S. Bhattacharya, K. Hatua, "A unified control scheme for harmonic elimination in the front end converter of a 13.8 kV, 100 kVA transformerless intelligent power substation grid tied with LCL filter", in *Proc. IEEE Twenty-Ninth Annual Appl. Power Electron. Conf. Expo.(APEC)*, 2013, pp.964-971.

[10] Zhou Yan, Duan Shanxu, Liu Fei, Yin Jinjun, "Research on digital implementation of proportional-resonant controller based on a three-phase PV grid-connected system," *Electrical Machines and Systems (ICEMS), ICEMS 2008,* pp. 2746–2749, 2008.